Catalysis Today 171 (2011) 221–228

Contents lists available at ScienceDirect

Catalysis Today

journal homepage: www.elsevier.com/locate/cattod

Comparative study of MTO conversion over SAPO-34, H-ZSM-5 and H-ZSM-22: Correlating catalytic performance and reaction mechanism to zeolite topology

Jinzhe Li, Yingxu Wei, Guangyu Liu, Yue Qi, Peng Tian, Bing Li, Yanli He, Zhongmin Liu*

National Engineering Laboratory for Methanol to Olefins, Dalian Institute of Chemical Physics, Chinese Academy of Sciences, 457 Zhongshan Road, Dalian, 116023, PR China

ARTICLE INFO

Article history:
Received 30 October 2010
Received in revised form 20 February 2011
Accepted 23 February 2011
Available online 30 March 2011

Keywords:
ZSM-22
Methanol
Ethene
Propene
MTO

ABSTRACT

Conversion of methanol to olefins (MTO) was comparatively studied over three zeolites with different topologies, *i.e.* SAPO-34, H-ZSM-5 and H-ZSM-22. The correlation between reaction mechanism and the zeolite topology was also investigated. SAPO-34 presented the highest selectivity for light olefins such as ethene and propene, and no aromatics were detected. H-ZSM-5 showed relatively high selectivity for ethene and propene, and large amount of aromatics were detected. Over H-ZSM-22, the selectivity for ethene is very low and a large amount of non-aromatic C_6^+ olefins generated. With the aid of ^{12}C-methanol/^{13}C-methanol switch technique, the reaction routes followed by methanol conversion over the three catalysts could be distinguished. The reaction mechanisms, which varied with the zeolite topologies, caused the differences in catalytic performances. The co-reaction of ^{13}C-methanol with ^{12}C-olefin or ^{12}C-aromatic, were carried out for further clarification of the operation of the different catalytic cycles in methanol conversion.

1. Introduction

Methanol-to-olefins (MTO) conversion is a very important process for the production of light olefins, such as ethene and propene, from alternative and abundant resources of natural gas or coal. Considerable effort has been devoted to the improvement of the catalyst performances and the process development [1–3]. Recently, the world's first commercial MTO unit, with a production capacity of 600,000 tons of lower olefins per year, was proved to be completely successful in its first commissioning operation [4]. In parallel with the process development, numerous research works have been done to elucidate the reaction mechanism of MTO conversion [5–8] and more than 20 mechanisms have been proposed by different researchers [1]. Among the proposed mechanisms, an indirect mechanism, hydrocarbon pool mechanism, which was firstly proposed by Kolboe and co-workers based on the experiments of the MTO conversion over SAPO-34 (CHA type: containing large cages and narrow 8-member ring openings [9]), attracted much more attention [10–12]. According to the hydrocarbon pool mechanism, the reaction cycle involved the methylation of "hydrocarbon pool intermediates" confined in the cages of SAPO-34 by methanol and subsequent elimination of ethene, propene, and butenes from the intermediates. Later, detailed studies revealed that the polymethylbenzenes composed largest part of the materials retained in the catalyst and that hexamethylbenzene was the most active species for methanol to olefin conversion [13–15]. Haw and co-workers proposed that the conversion of methanol over ZSM-5 (MFI type: containing crossed 10-member ring channels and channel intersections [9]) also follows the hydrocarbon pool mechanism [16,17], which was supported by Hunger and co-workers [18,19].

Furthermore, a work by Cui and co-workers [20] reported that the MTO conversion could only take place on zeolites that allow the hydrocarbon pool mechanism to work, and that due to the transition-state shape selectivity, MTO conversion over ZSM-22 (TON type: one-dimensional channels with 10-member ring openings [9]) could only produce dimethylether as the product. They also found that ZSM-22 displayed a low but appreciable production of olefins at the beginning of methanol conversion, but they believed that the initial conversion resulted from the impurity phase (ZSM-11) and/or the external acid sites [20].

However, hydrocarbon pool mechanism might not be the only one that MTO reactions follow. Because the olefins were the main products of this reaction and the olefins methylation or cracking reactions over zeolite catalysts have been suggested and proved by several research groups [21–23], methanol might be converted to olefins through the mechanism other than aromatic based hydrocarbon pool mechanism, *i.e.* the olefin methylation-cracking reaction cycle. In fact, over H-ZSM-5, Svelle and Bjorgen [24,25] have found that the reaction proceeded through dual-cyclic reaction cycle. Ethene was formed through the reaction route following hydrocarbon pool mechanism with lower methylated benzene as reactive intermediates, and apart from that, the olefin methylation-cracking cycle was responsible for the formation of

* Corresponding author. Tel.: +86 411 84685510; fax: +86 411 84691570.
E-mail address: liuzm@dicp.ac.cn (Z. Liu).

0920-5861/$ – see front matter © 2011 Elsevier B.V. All rights reserved.
doi:10.1016/j.cattod.2011.02.027

propene, butenes and higher olefins. This suggests that if the hydrocarbon pool mechanism were suppressed, methanol conversion over H-ZSM-22 might proceed through the methylation-cracking route. Our previous work on the methanol conversion over H-ZSM-22 showed that nearly complete conversion of methanol could be obtained over H-ZSM-22 at 450 °C (WHSV = 10 h^{-1}) [26]. In a report from the group of Olsbye [27], they also found that under suitable conditions H-ZSM-22 has the conversion capacity comparable to that of SAPO-34. These results have been somewhat contradictive with the report of Cui et al. [20]. Further study on the MTO reaction over H-ZSM-22 is necessary, especially on the reaction mechanism. Just before the submission of our manuscript, a paper focused on the reaction mechanism over H-ZSM-22 has been published by Olsbye and co-workers [28].

In the present study, methanol conversion over H-ZSM-22 was studied with ^{13}C labeling technique with the comparison of that over H-ZSM-5 and SAPO-34 under the identical reaction conditions. To clarify the role of the two catalytic cycles (mentioned by Svelle and Bjorgen [24,25]) in methanol conversion over these three zeolites with different topology, the co-reaction of ^{13}C-methanol and unlabeled olefin/aromatic were also studied.

2. Experimental

2.1. Catalyst preparation

SAPO-34 was synthesized hydrothermally using triethylamine as the template [29–32]. Pseudoboehmite, orthophosphoric acid and colloidal silica were used as the sources of aluminum, phosphorus and silicon, respectively. The chemical compositions of starting gels were 1.0 Al_2O_3: 1.0 P_2O_5: 0.6 SiO_2: 3 NEt_3: 50 H_2O, which were prepared as follows. Pseudoboehmite was added to vigorously stirred water in a glass beaker and then phosphoric acid was added. After stirring for a determined time, colloidal silica was added to this mixture, which was then stirred for a further half hour before triethylamine was added. The resulting gel was then transferred to a Teflon-lined stainless steel autoclave. The crystallization was carried out at 200 °C under autogenously pressure. The H-SAPO-34 was obtained by the calcination of the crystallized products at 550 °C for 4 h.

ZSM-5 (SiO_2/Al_2O_3 = 95) was purchased from Nanda Catalyst Co., Ltd. The protonic form ZSM-5 was obtained by calcination of the ammonium form sample at 550 °C for 4 h. The sample of ZSM-22 (SiO_2/Al_2O_3 = 69) was kindly provided by another group of Dalian Institute of Chemical Physics. The NH_4-ZSM-22 was obtained by ion-exchanging the calcined solid with the solution of ammonium nitrate. After the ion-exchange, the sample was washed with deionized water, dried at 110 °C and finally calcined at 550 °C for 4 h to achieve H-ZSM-22.

2.2. Characterization

The crystallinity and phase purity of the samples was characterized by powder X-ray diffraction (RIGAKU D/max-rb powder diffractometer) with Cu $K\alpha$ radiation.

The acidity of the catalysts was determined by temperature programmed desorption of ammonia (NH_3-TPD). A catalyst sample of 0.14 g was loaded into a U-shaped micro-reactor and pre-treated at 650 °C for 30 min in a flow of helium. After the pre-treatment, the sample was cooled to 100 °C and saturated with ammonia. The temperature was increased from 100 to 600 °C at a constant heating rate of 10 °C/min under a He flow of 40 mL/min. The concentration of ammonia in the exit gas was monitored continuously with a TCD detector.

2.3. Methanol conversion

Methanol conversion was performed in a fixed-bed quartz tubular reactor at atmospheric pressure. For pulse reactions, a catalyst sample of 45 mg (60–80 mesh) was loaded into the reactor. The reactor was heated to reaction temperature and maintained for 1 h before reaction. Then an injection of methanol of 1 μL was conducted onto the catalyst, and the effluent was kept warm and analyzed by online gas chromatography (Varian GC3800) equipped with a PoraPLOT Q-HT capillary column and a FID detector. In the ^{13}C labeling experiments, pre-reaction of 15 pulses of ^{12}C-methanol was performed and that was followed by successive pulses of ^{13}C-methanol. The effluent products of each ^{13}C-methanol pulse reaction were collected and analyzed by Agilent 6890/5973N MSD GC–MS. For the co-reaction of ^{13}C-methanol and unlabeled olefin/aromatic, only one pulse of reactants mixture was injected onto the catalyst bed at 450 °C and then the effluent was analyzed by GC-MS. The molar ratio of ^{13}C-methanol to unlabeled reactant was 20. In the co-reaction of ^{13}C-methanol and butene, 1-butanol was used as the reactant which was easily converted into butene in situ.

3. Results and discussion

MTO conversions over different type of zeolites were performed on the pulse reaction system using ^{13}C labeling technique and the results were displayed in Tables 1–3 and Figs. 1–4. For comparison, all the reactions were carried out at 450 °C with reactant-catalyst contact time of 0.08 s. The conversion in the context was referred to the percent of methanol which were converted into hydrocarbons, that is to say, dimethylether was also considered as reactant in the following discussion.

In Table 1, when the first methanol injection was conducted onto SAPO-34 catalyst, the methanol conversion was 40.4%. After 15 injections of methanol, the conversion increased to 91.6%. This presented the performance difference in the induction period and steady-state period of MTO over SAPO-34. It is interesting to

Table 1
Methanol conversion and product selectivity of MTO over SAPO-34.

Pulse number	Conversion (%)	Selectivity (C%)							
	CH_3OH	C_1^0	$C_2^=$	C_2^0	$C_3^=$	C_3^0	C_4	C_5	C_6^+
1	40.4	3.5	6.6	0.0	60.8	1.3	15.6	7.6	4.7
15	91.6	0.8	26.8	0.2	42.4	6.8	16.0	5.8	1.2
19	96.0	0.8	27.3	0.2	44.1	4.0	16.0	6.3	1.4

Table 2
Methanol conversion and product selectivity of MTO over ZSM-5.

Pulse number	Conversion (%)	Selectivity (C%)							
	CH_3OH	C_1^0	$C_2^=$	C_2^0	$C_3^=$	C_3^0	C_4	C_5	C_6^+
1	76.0	1.8	8.4	0.0	37.3	1.4	15.4	11.1	24.6
15	82.5	2.2	10.8	0.1	36.2	1.2	14.9	8.6	26.0
19	78.5	2.0	9.1	0.1	37.1	1.1	14.5	10.6	25.5

Table 3
Methanol conversion and product selectivity of MTO over ZSM-22.

Pulse number	Conversion (%)	Selectivity (C%)							
	CH_3OH	C_1^0	$C_2^=$	C_2^0	$C_3^=$	C_3^0	C_4	C_5	C_6^+
1	76.5	2.3	3.7	0.4	22.3	3.4	17.2	28.6	22.1
2	66.8	1.8	3.0	0.3	20.2	3.9	16.9	28.4	25.5
5	63.7	2.1	3.0	0.3	19.6	3.4	16.3	28.7	26.6
15	53.7	2.5	3.0	0.3	19.3	3.2	15.8	27.8	28.1
19	40.4	3.3	3.0	0.2	20.0	2.7	15.7	27.8	27.3

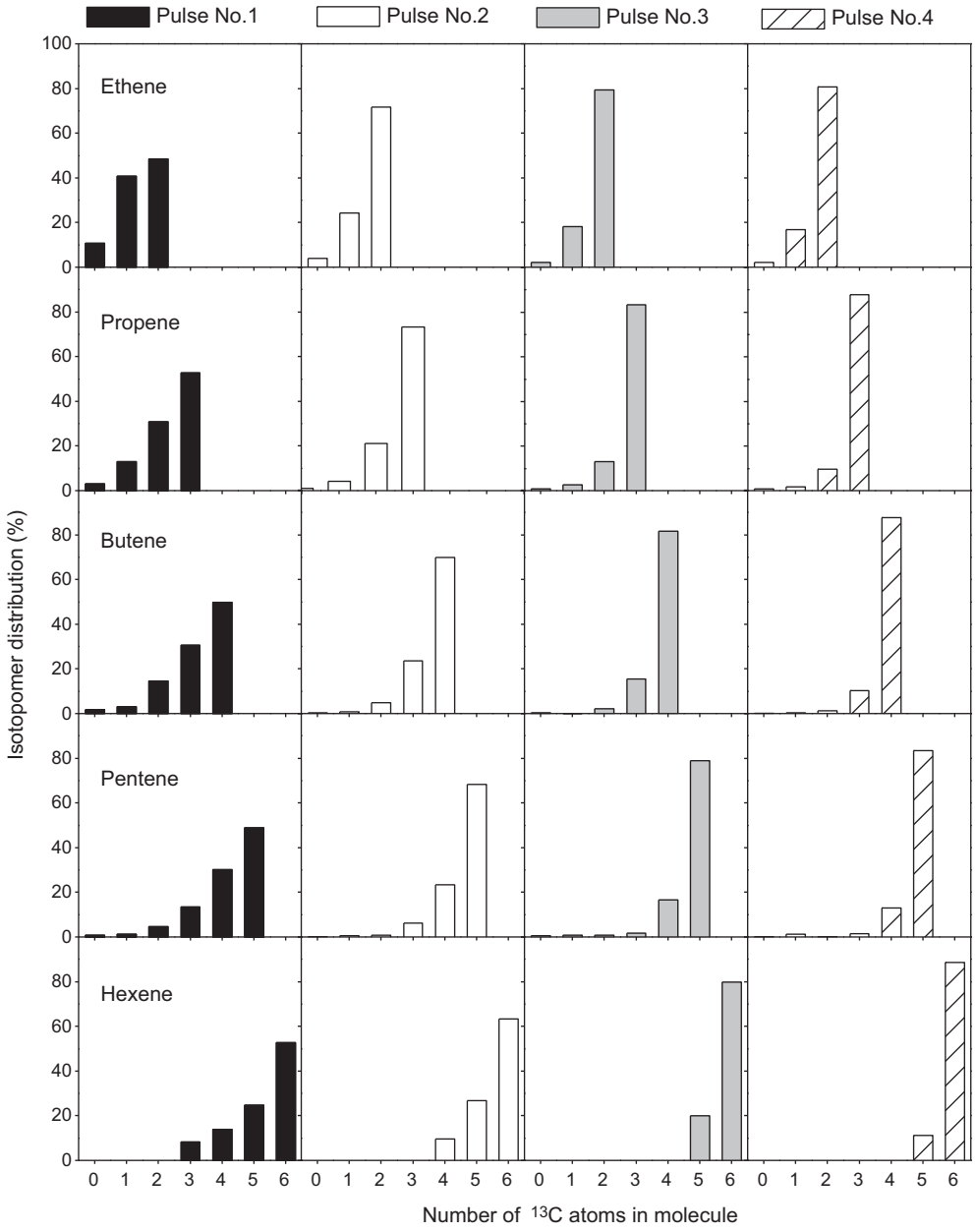

Fig. 1. Isotopic distribution of the effluent products of successive ^{13}C-methanol pulse reaction over SAPO-34 at 450 °C after the pre-reaction of 15 pulses of ^{12}C-methanol, CT = 0.08 s.

observe the variation of product distribution with the consecutive methanol injections. The first methanol injection gave rise to extremely high propene selectivity (60.8%), while ethene selectivity was very low (6.6%). The higher olefins (C_6^+) selectivity accounts for 4.7% of methanol conversion, and the methane and propane selectivity were 3.5% and 1.3%, respectively. With the further conduction of methanol pulses, the selectivities to propene, C_6^+ and methane decreased, meanwhile the ethene and propane selectivity increased.

There was still an ongoing debate on the real reason of the changes in product selectivity (especially for ethene and propene) with the progress of MTO reaction over SAPO-34. Chen et al. [33] stated that the free space of the cages was reduced by coke deposition and the formation of larger molecules via larger intermediates was suppressed, which means that the transition-state shape selectivity determined the product distribution. This can be used to explain the enhancement of ethene selectivity with methanol conversion and coke deposition, but it is contradictive with the appearance of extremely high propene selectivity from the first methanol injection. In a recent report, Olsbye and co-workers [34] argued that the product shape selectivity dominates the MTO reaction over SAPO-34, and this cannot also explain the significant differences between the product distribution of the first methanol pulse and that of the 15–19th methanol pulse over SAPO-34 (as shown in Table 1). The mechanism of olefin formation during the induction period and the steady state period might be different.

After 15 pulses of ^{12}C-methanol were performed, 4 pulses of the ^{13}C labeling methanol were injected into reactor successively, and the isotopic distribution in the effluent of each pulse was analyzed by GC–MS and displayed in Fig. 1.

All of the products contained ^{12}C atoms and ^{13}C atoms. The product molecules containing only ^{13}C atoms were about 50% when the first pulse of ^{13}C-methanol was injected. The second and third ^{13}C methanol injection induced a rapid increase of the products con-

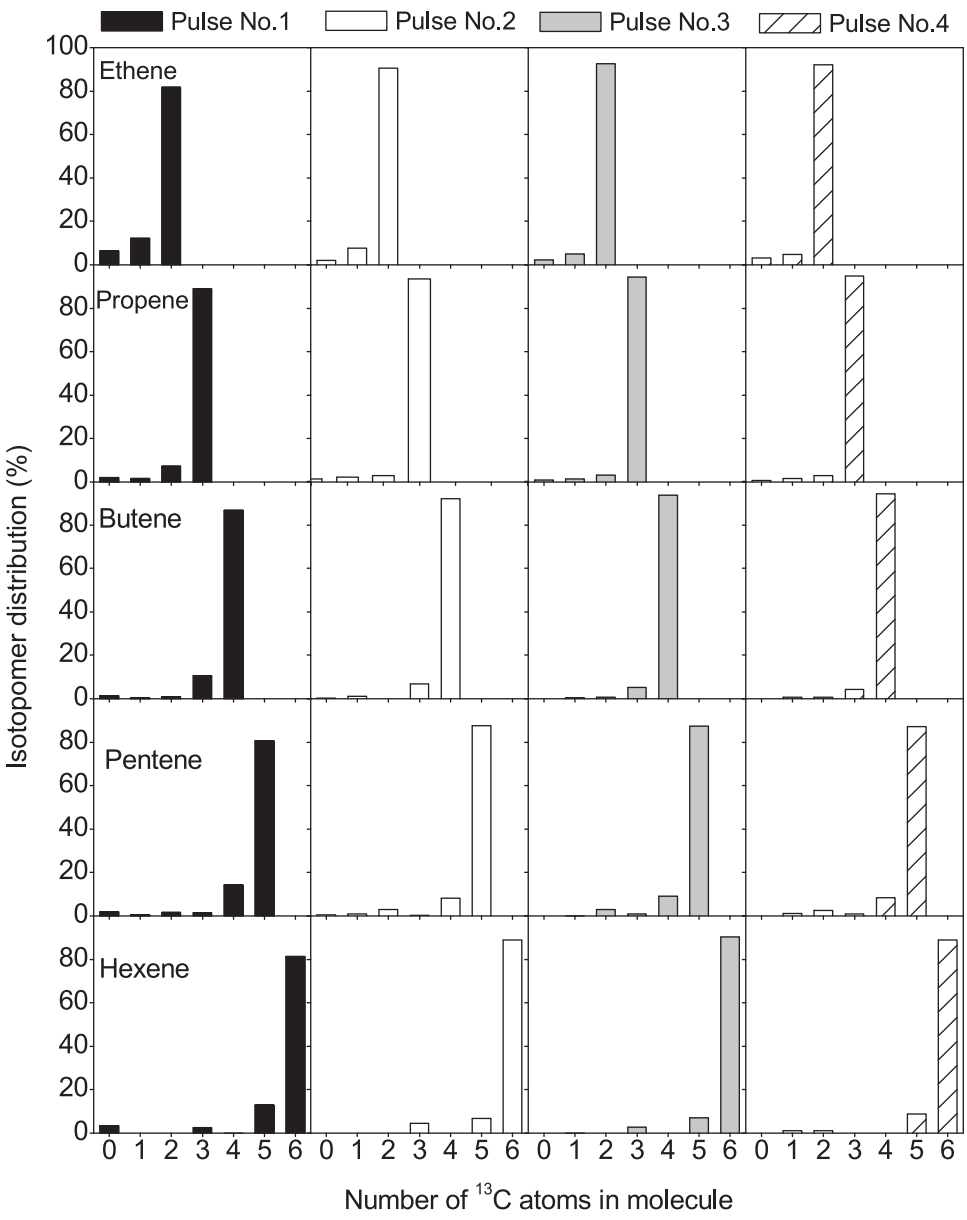

Fig. 2. Isotopic distribution in the effluent products of successive ^{13}C-methanol pulse reaction over ZSM-5 at 450 °C after the pre-reaction of 15 pulses of ^{12}C-methanol, CT = 0.08 s.

taining only ^{13}C atoms. When the fourth pulse of ^{13}C-methanol was injected, the proportion of the molecules containing only ^{13}C atoms exceeded 80% in the product isotopic distribution. The total ^{13}C contents of the main products over SAPO-34 were shown in Fig. 4 and will be discussed later together with the results over ZSM-5 and ZSM-22.

Table 2 shows the results of MTO reaction over ZSM-5. First injection gave rise to the conversion of 76%. Propene was the main product with a selectivity of about 37%, and the ethene selectivity was about 10%. The selectivity for C_6^+ over ZSM-5 was about 25%, which consisted mostly of toluene and xylene (not shown in the Table).

The pulse reaction of ^{13}C methanol was also performed successively over ZSM-5 after the pre-reaction of 15 pulses of ^{12}C-methanol, and the isotopic distribution in the effluent was shown in Fig. 2. The results were very different from those over SAPO-34. The proportion of the product molecule containing only ^{13}C atoms was 80% for the first injection of ^{13}C methanol upon the pre-reacted H-ZSM-5, which is largely higher than that over SAPO-34. The molecules containing only ^{13}C atoms also increased with the further injection of ^{13}C methanol as those over SAPO-34.

Table 3 gives the results of the methanol conversion over ZSM-22 performed under the similar reaction conditions as those used over SAPO-34 and ZSM-5. The methanol conversion was 76.5% for the first methanol injection and decreased with the methanol pulse number. After 19 injections of methanol were conducted, methanol conversion was 40.4%. Propene was one of the main products with a selectivity of ~20%, while very low ethene selectivity (only 3%) was observed. The selectivities for C_5 and C_6^+ were in the range of 22%–29% and most of the C_6^+ hydrocarbons were olefins.

In comparison of SAPO-34 and ZSM-5, the performance of methanol transformation over ZSM-22 showed the differences in methanol conversion and product generation. Over SAPO-34 and ZSM-5, almost no deactivation occurred even after 19 pulses of methanol injections. However, the deactivation was observed over ZSM-22 since the second methanol injection. About the relatively rapid deactivation of ZSM-22, it was proposed that the channel openings of ZSM-22 (TON type zeolite with only 1-dimensional

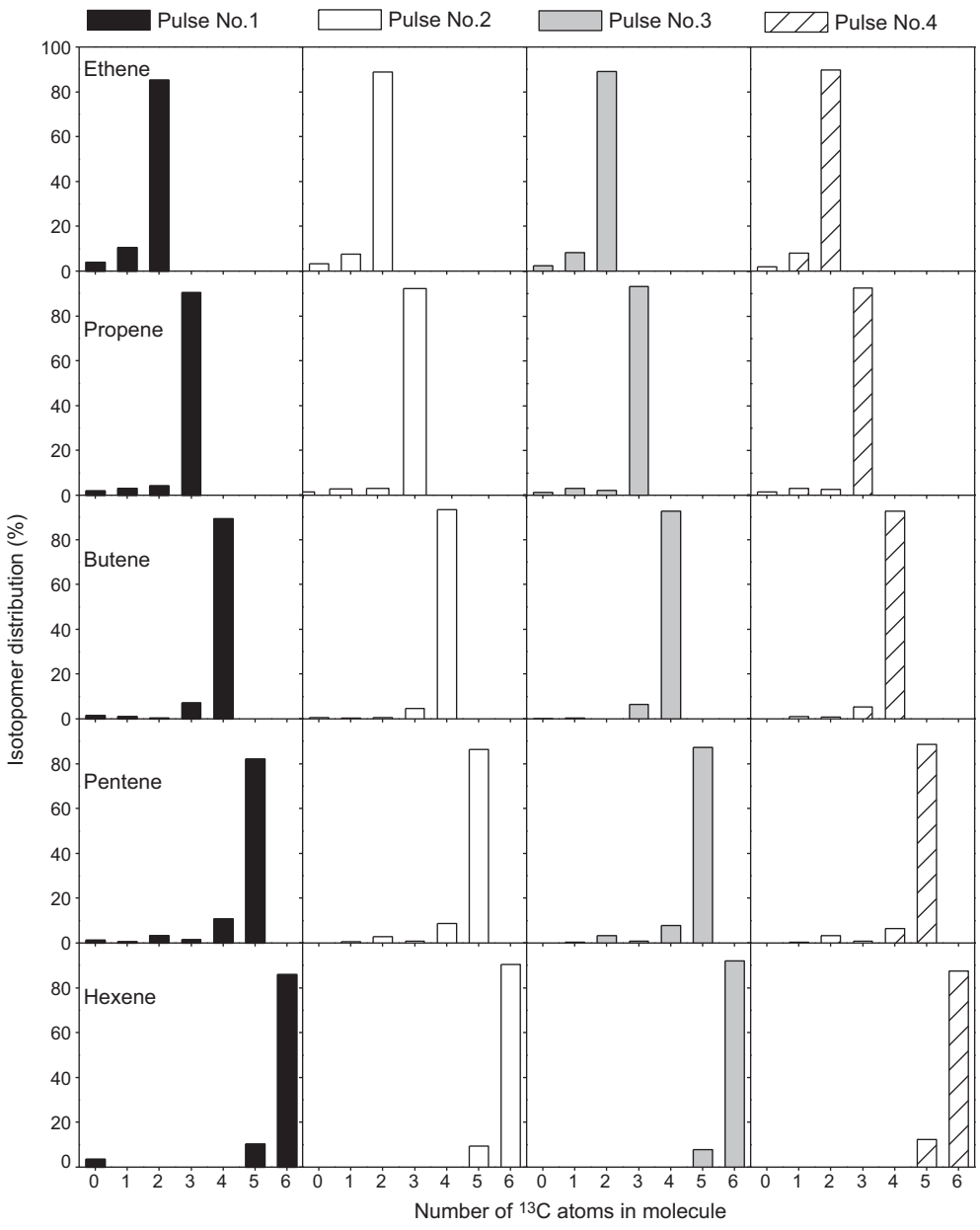

Fig. 3. Isotopic distribution in the effluent products of successive ^{13}C-methanol pulse reaction over ZSM-22 at 450 °C after the pre-reaction of 15 pulses of ^{12}C-methanol, CT = 0.08 s.

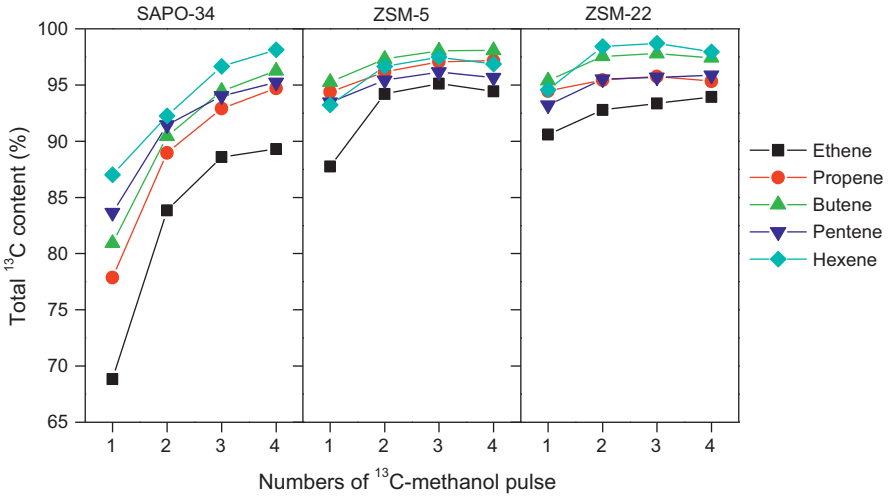

Fig. 4. Total ^{13}C content in the effluent products of successive ^{13}C-methanol pulse reaction at 450 °C after the pre-reaction of 15 pulses of ^{12}C-methanol, CT = 0.08 s.

channels) were easy to be blocked by the coke species, and this might be responsible for the deactivation. The location of these coke species in the catalyst was still unknown. Some researchers [25,35–38] argued that ZSM-5 (MFI type with 10 member ring and intersections) cannot provide enough spaces for the formation of coke species larger than tetramethylbenzenes, and this was believed to be the reason of the long life time of ZSM-5 for methanol conversion. The deactivation of ZSM-5 was caused by the coke on the external surface of the zeolite crystals [35]. The diameter of ZSM-22 channels was close to that of ZSM-5. So the formation of the large coke species in the channels might also be suppressed. But large coke species may form on the external surface or near the pore mouth. These species could age to insoluble graphitic species or be adsorbed in the channels (or near the pore mouth) and then blocked the pore openings. Among the three catalysts, ZSM-22 has the highest selectivity for C_5. Although the C_6^+ selectivity over ZSM-22 was comparable with that over ZSM-5, the composition was very different. Over ZSM-5 the aromatics constituted the main part of C_6^+, while olefins dominated over ZSM-22.

After 15 pulses of ^{12}C-methanol pre-injection, ^{13}C methanol pulse reaction was also conducted and the isotopic distribution indicated hydrocarbon products containing only ^{13}C atoms was predominant (>80%) in the effluent and its proportion of ^{13}C-containing products increased with the further ^{13}C-methanol injection. These observations were similar to those over ZSM-5 and reflected the reaction over the two zeolites possibly followed a close reaction mechanism.

Different from the publications [24,25], the isotopic switch experiments in this study were performed on the pulse reaction system. In this setup, the mixing of ^{12}C-methanol and ^{13}C-methanol was avoided and the switch of $^{12}C/^{13}C$ could be clear-cut and an immediate products analysis after isotopic switch could be realized. This also makes it possible to correlate the differences in the ^{13}C distribution to the reaction mechanism. ^{12}C-methanol pre-reaction generated ^{12}C-polymethylbenzenes in the cages or channels of the catalysts. The incorporation of ^{12}C atom into the products would predict that these ^{12}C-polymethylbenzenes worked as the reaction center in methanol-to-olefin conversion, and the reaction followed hydrocarbon pool mechanism [5,6]. Through another reaction route proposed for methanol conversion, olefin methylation-cracking [24,25] without involving the ^{12}C-polymethylbenzenes retained in the catalysts, the products generation would be independent of the scrambling of ^{12}C atoms. However, if both of the two reaction mechanisms were allowed to operate on a specific catalyst, the products from the former reaction route would possibly serve as the initial olefins for the later reaction route, which makes the reaction route determination more difficult from the isotopic distribution. Anyway, the observations in the above-mentioned ^{13}C switch experiments are still helpful for distinguishing the reaction route of methanol conversion over the three catalysts, even the conclusion is difficult to be drawn exactly.

The total ^{13}C contents in the products of methanol conversion over different catalysts were calculated from the detailed isotopic distribution and plotted in Fig. 4 against the pulse number of ^{13}C methanol. Among the three catalysts studied, ^{12}C atoms incorporation is more predominant over SAPO-34 than ZSM-5 and ZSM-22, especially in ethene. This indicates that the hydrocarbon pool mechanism is the main reaction route over SAPO-34, especially for ethene formation. In the report of [34], the authors performed the $^{12}C/^{13}C$ switch experiments over SAPO-34 on the continuous-flow reaction system, and they found that the ^{13}C contents of ethene, propene and butenes were very similar. However, in the present work, ethene formation after $^{12}C/^{13}C$ switch presented evident difference in the ^{13}C contents of products. As shown in Fig. 4, the total ^{13}C content of ethene was always lower than that of other products. This finding suggested that even over SAPO-34, part of the higher olefins (>C_3) might be formed through the olefin methylation-cracking route. This can also explain the extremely high propene selectivity over SAPO-34 at the first methanol pulse. During the induction period the active hydrocarbon pool species in SAPO-34 were relatively rare, and the reaction occurred more possibly followed olefin methylation-cracking route. This was responsible for the relatively higher propene selectivity obtained during the induction period.

The incorporation of ^{12}C atoms into the products over ZSM-5 was less obvious than that over SAPO-34, but ethene shows appreciable incorporation of ^{12}C atoms. These observations were consistent with the work of Svelle and Bjorgen [24,25] and predicted that the olefin methylation-cracking mechanism was also one of the main reaction routes for the formation of C_3^+ olefins over ZSM-5. But ethene was formed mainly from the reaction following hydrocarbon pool mechanism.

The incorporation of ^{12}C atoms into C_3^+ olefins of methanol conversion was even weakened by using ZSM-22 as catalyst. At the 2^{nd} to 4^{th} injection of ^{13}C methanol, the total ^{13}C contents of propene, butene, pentene and hexene were higher than 95%. As shown in Table 3, C_3^+ olefins were the main products of methanol conversion over ZSM-22, it was reasonable to propose that olefin methylation-cracking route is operative for methanol conversion over ZSM-22. The incorporation of ^{12}C atoms into ethene over ZSM-22 was higher than that into C_3^+ olefins. This suggested that over ZSM-22 the ethene might be also formed mainly from hydrocarbon pool mechanism, as which was formed over ZSM-5. However, the very low selectivity for ethene was observed over ZSM-22 indicating methanol conversion with hydrocarbon pool mechanism was suppressed.

The differences in the product distribution over ZSM-22 and ZSM-5 can be explained by taking the zeolite topology into account. ZSM-22 has only one dimensional 10-member ring channels with no intersections., so the largest space which ZSM-22 can offer was $5.7 \times 4.6\ Å^2$. ZSM-5 also has the 10-member ring channels but it contains channel intersections which can accommodate cyclic species as hydrocarbon pool. Actually, large amount of toluene and xylene were detected among C_6^+ products over ZSM-5. However, linear olefins accounted for the largest part of C_6^+ over ZSM-22. From the point of reaction mechanism, the channels of ZSM-22 sterically hindered the reaction following the mechanism of hydrocarbon pool, and methanol conversion mainly go through the olefin methylation and cracking route. This could explain the very low selectivity of ethene over ZSM-22. For clarity, the reaction routes of methanol conversion over the three zeolites with different pore structures were illustrated in Fig. 5.

To further evaluate the importance of the above-mentioned two catalytic cycles over these three catalysts, the co-reaction of ordinary olefin (1-butene) or aromatic (p-xylene) with ^{13}C labeled methanol was studied. The molar ratio of unlabeled reactant to ^{13}C-methanol was about 1/20. The co-reactions were carried out at 450 °C with contact time of 0.04 s. In the co-reaction of ^{13}C-methanol and 1-butene, 1-butene was produced by 1-butanol in situ. The co-reaction results were shown in Fig. 6. Over SAPO-34, the ^{13}C contents of the effluents in the co-reaction of ^{13}C-methanol and ^{12}C-p-xylene were higher than 95%. By contrast, relatively low ^{13}C content of the products (especially heavier olefins) was presented in the co-reaction of ^{13}C-methanol and ^{12}C-butene over SAPO-34. These differences indicated that the added ^{12}C-p-xylene molecules had no involvement in methanol conversion due to the larger molecular size than the pore diameter of SAPO-34. The appearance of ^{12}C atoms from the added ^{12}C-butene molecules in the products implied the participation of butene in the reaction and higher olefins might be formed through the olefin methylation-cracking reaction route, which is consistent with the work of pulse reaction over SAPO-34.

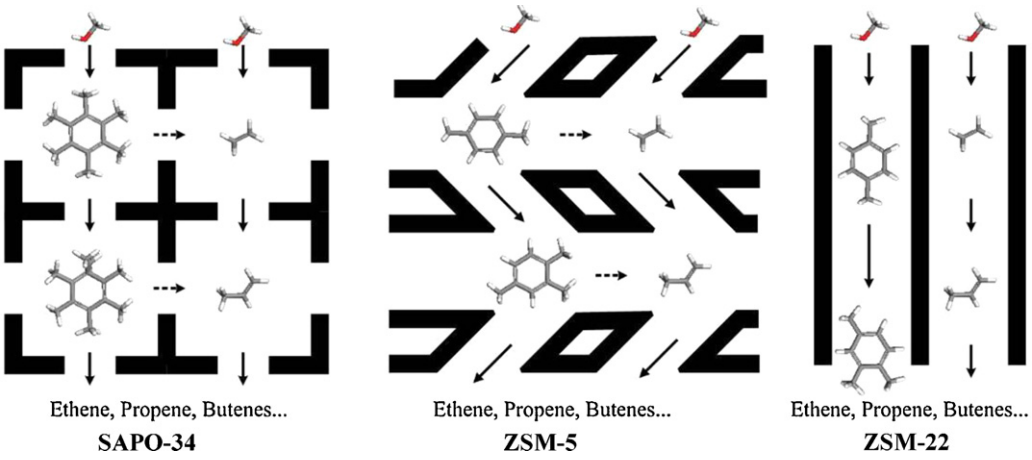

Fig. 5. Illustration of reaction routes of methanol conversion over zeolites with different pore structures.

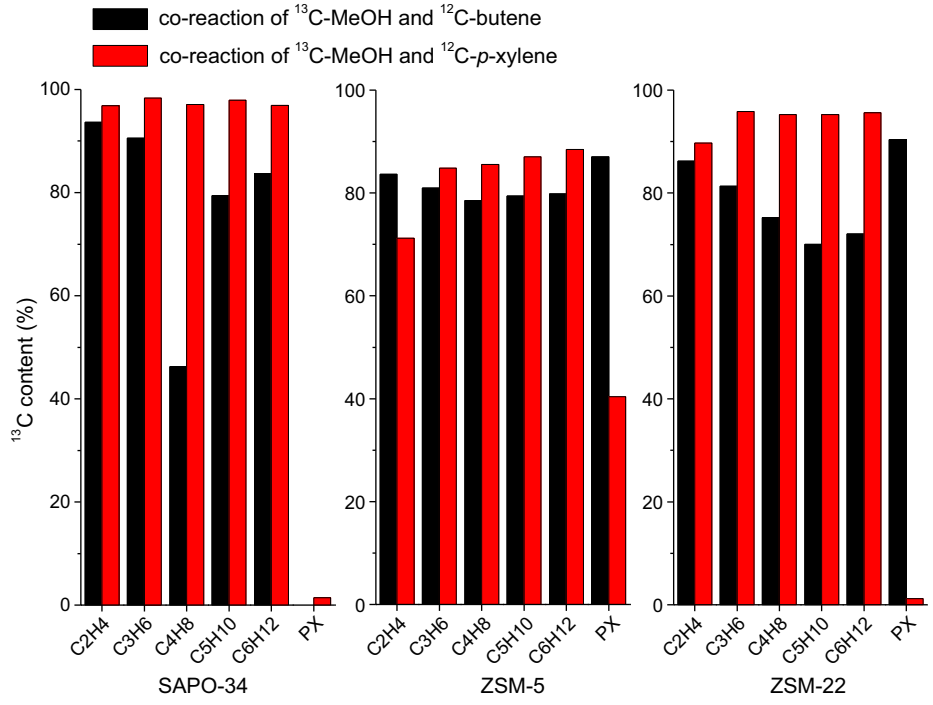

Fig. 6. ^{13}C content in the effluent products of co-reaction of ^{13}C-methanol and ^{12}C-butene or ^{12}C-p-xylene over zeolites with different pore structures. (T = 450 °C, CT = 0.04 s, ^{13}C-methanol/unlabeled reactant (molar ratio) = 20/1.).

When co-reactions of ^{13}C-methanol with ^{12}C-p-xylene or ^{12}C-butene were carried out over ZSM-5, ^{12}C-p-xylene addition gave rise to the low ^{13}C content of ethene while ^{12}C-butene addition resulted in the low ^{13}C content of higher olefins (propene, pentene and hexene). This implies that both ^{12}C-p-xylene and ^{12}C-butene were involved in the formation of olefin products over ZSM-5, but their involvement worked in different way. Ethene formation from the reaction following hydrocarbon pool mechanism could be improved by the co-feeding of xylene, however the formation of higher olefins, mainly from the methylation-cracking cycle, were more possibly beneficial from the olefin addition.

Over ZSM-22, in the co-reaction of ^{13}C-methanol with ^{12}C-p-xylene, the ^{13}C content of ethene was still the lowest but olefins heavier than propene presented relatively high ^{13}C content (95%), indicating that the added ^{12}C-p-xylene did not involve in the higher olefins formation over ZSM-22. In the co-reaction of ^{13}C-methanol with ^{12}C-butene, the ^{13}C content of all the olefins were lower than that in the co-reaction with ^{12}C-p-xylene. These results suggest that the olefin methylation-cracking reaction cycle were more important for MTO reaction over ZSM-22 than that over SAPO-34 and ZSM-5.

4. Conclusions

The reaction mechanisms of MTO over zeolites were very complex. Methanol conversion may follow aromatic based hydrocarbon pool mechanism and olefin methylation-cracking mechanism. The results in ^{13}C-labeling pulse experiments indicated that reaction route of methanol conversion could be altered through the space confinement from the zeolite with different structure topologies, due to the differences in space requirements of the two mechanisms. Aromatic based hydrocarbon pool mechanism was the most important reaction route of methanol conversion over SAPO-34 with enough spaces for the accommodation of large intermediates.

Methanol conversion catalyzed by ZSM-5 both followed the hydrocarbon pool mechanism and the olefin methylation-cracking route. Over the zeolite with 1-dimensional 10-member ring channels, H-ZSM-22, different from the report by Cui et al. [19], the present work suggested that methanol could be converted into olefins, and that owing to the absence of supercages or channel intersections for hydrocarbon pool formation, the olefin methylation-cracking cycle was the main reaction route of methanol conversion. Aromatics or olefins addition could improve the methanol conversion following hydrocarbon pool mechanism or methylation-cracking route respectively.

Acknowledgments

The authors thank the Natural Science Foundation of China (no.20903091 and no. 20973164) for financial support.

Appendix A. Supplementary data

Supplementary data associated with this article can be found, in the online version, at doi:10.1016/j.cattod.2011.02.027.

References

[1] M. Stocker, Micropor. Mesopor. Mater. 29 (1999) 3–48.
[2] F.J. Keil, Micropor. Mesopor. Mater. 29 (1999) 49–66.
[3] Z.M. Liu, C.L. Sun, G.W. Wang, Q.X. Wang, G.Y. Cai, Fuel Process Technol. 62 (2000) 161–172.
[4] http://english.cas.cn/ST/BR/br_progress/201008/t20100811_57273.shtml.
[5] U. Olsbye, M. Bjorgen, S. Svelle, K.P. Lillerud, S. Kolboe, Catal. Today 106 (2005) 108–111.
[6] J.F. Haw, W.G. Song, D.M. Marcus, J.B. Nicholas, Acc. Chem. Res. 36 (2003) 317–326.
[7] W. Wang, M. Hunger, Acc. Chem. Res. 41 (2008) 895–904.
[8] D. Lesthaeghe, V. Van Speybroeck, G.B. Marin, M. Waroquier, Ind. Eng. Chem. Res. 46 (2007) 8832–8838.
[9] http://www.iza-structure.org/databases/.
[10] I.M. Dahl, S. Kolboe, J. Catal. 149 (1994) 458–464.
[11] I.M. Dahl, S. Kolboe, Catal. Lett. 20 (1993) 329–336.
[12] I.M. Dahl, S. Kolboe, J. Catal. 161 (1996) 304–309.
[13] W.G. Song, J.F. Haw, J.B. Nicholas, C.S. Heneghan, J. Am. Chem. Soc. 122 (2000) 10726–10727.
[14] B. Arstad, S. Kolboe, J. Am. Chem. Soc. 123 (2001) 8137–8138.
[15] B. Arstad, S. Kolboe, Catal. Lett. 71 (2001) 209–212.
[16] P.W. Goguen, T. Xu, D.H. Barich, T.W. Skloss, W.G. Song, Z.K. Wang, J.B. Nicholas, J.F. Haw, J. Am. Chem. Soc. 120 (1998) 2650–2651.
[17] D.M. McCann, D. Lesthaeghe, P.W. Kletnieks, D.R. Guenther, M.J. Hayman, V. Van Speybroeck, M. Waroquier, J.F. Haw, Angew. Chem. Int. Ed. 47 (2008) 5179–5182.
[18] M. Seiler, W. Wang, A. Buchholz, M. Hunger, Catal. Lett. 88 (2003) 187–191.
[19] W. Wang, Y.J. Jiang, M. Hunger, Catal. Today 113 (2006) 102–114.
[20] Z.M. Cui, Q. Liu, W.G. Song, L.J. Wan, Angew. Chem. Int. Ed. 45 (2006) 6512–6515.
[21] S. Svelle, P.A. Ronning, S. Kolboe, J. Catal. 224 (2004) 115–123.
[22] S. Svelle, P.O. Ronning, U. Olsbye, S. Kolboe, J. Catal. 234 (2005) 385–400.
[23] Z.M. Cui, Q. Liu, Z. Ma, S.W. Bian, W.G. Song, J. Catal. 258 (2008) 83–86.
[24] S. Svelle, F. Joensen, J. Nerlov, U. Olsbye, K.P. Lillerud, S. Kolboe, M. Bjorgen, J. Am. Chem. Soc. 128 (2006) 14770–14771.
[25] M. Bjorgen, S. Svelle, F. Joensen, J. Nerlov, S. Kolboe, F. Bonino, L. Palumbo, S. Bordiga, U. Olsbye, J. Catal. 249 (2007) 195–207.
[26] J.Z. Li, Y. Qi, Z.M. Liu, G.Y. Liu, D.Z. Zhang, Catal. Lett. 121 (2008) 303–310.
[27] S. Teketel, S. Svelle, K.-P. Lillerud, U. Olsbye, ChemCatChem 1 (2009) 78–81.
[28] S. Teketel, U. Olsbye, K.-P. Lillerud, P. Beato, S. Svelle, Micropor. Mesopor. Mater. 136 (2010) 33–41.
[29] J. Tan, Z.M. Liu, X.H. Bao, X.C. Liu, X.W. Han, C.Q. He, R.S. Zhai, Micropor. Mesopor. Mater. 53 (2002) 97–108.
[30] G.Y. Liu, P. Tian, J.Z. Li, D.Z. Zhang, F. Zhou, Z.M. Liu, Micropor. Mesopor. Mater. 111 (2008) 143–149.
[31] G.Y. Liu, P. Tian, Y. Zhang, J.Z. Li, L. Xu, S.H. Meng, Z.M. Liu, Micropor. Mesopor. Mater. 114 (2008) 416–423.
[32] D.Z. Zhang, Y.X. Wei, L. Xu, F.X. Chang, Z.Y. Liu, S.H. Meng, B.L. Su, Z.M. Liu, Micropor. Mesopor. Mater. 116 (2008) 684–692.
[33] D. Chen, A. Grlnvold, K. Moljord, A. Holmen, Ind. Eng. Chem. Res. 46 (2007) 4116–4123.
[34] B.P.C. Hereijgers, F. Bleken, M.H. Nilsen, S. Svelle, K.-P. Lillerud, M. Bjorgen, B.M. Weckhuysen, U. Olsbye, J. Catal. 264 (2009) 77–87.
[35] T. Behrsing, H. Jaeger, J.V. Sanders, Appl. Catal. 54 (1989) 289–302.
[36] M. Guisnet, L. Costa, F.R. Ribeiro, J. Mol. Catal. A: Chem. 305 (2009) 69–83.
[37] M. Guisnet, P. Magnoux, Appl. Catal. A: Gen. 212 (2001) 83–96.
[38] L. Palumbo, F. Bonino, P. Beato, M. Bjorgen, A. Zecchina, S. Bordiga, J. Phys. Chem. C 112 (2008) 9710–9716.